

S-PARAMETER MEASUREMENTS AND APPLICATIONS OF SUPERCONDUCTING FLUX FLOW TRANSISTORS

J. S. Martens, V. M. Hietala, T. E. Zipperian, D. S. Ginley, and C. P. Tigges
 Sandia National Laboratories, Department 1140, Albuquerque, NM 87185

Julia M. Phillips
 AT&T Bell Laboratories, 600 Mountain Avenue, Murray Hill, NJ 07974

ABSTRACT

We have performed microwave two-port S-parameter measurements and modelling on Superconducting Flux Flow Transistors (SFFTs). These transistors, based on the magnetic control of flux flow in an array of High Temperature Superconducting (HTS) weak links, can exhibit significant available power gain at microwave frequencies (over 20 dB at 7-10 GHz in some devices). The input impedance is largely inductive while the output impedance is resistive and inductive. The characteristics are such that these devices are potentially useful in numerous applications including matched amplifiers.

INTRODUCTION

The SFFT is a relatively recently developed active four terminal superconducting device (e.g.,(1)-(5)). The device exhibits very high speed operation (10-30 ps transit times with 3 μ m minimum feature size), large gain and impedance levels that are useful for many applications. The present work concentrates on small signal S-parameter measurements of these devices and a discussion of an SFFT application, matched amplifiers, that can be better analyzed employing this data.

DEVICE BASICS

The typical SFFT consists of a parallel array of weak superconducting links connecting two unweakened superconducting electrodes and a superconducting control line to provide a local magnetic field. An example of this structure is shown in Fig. 1. The links are typically 2-3 μ m wide by 10 μ m long and 50-90 nm thick (while the electrodes are at least 200 nm thick). The number of links does not strongly affect performance but larger numbers of links help by lowering output resistance and slightly increasing device gain at the expense of frequency response (5). When the device is biased below the critical current, typically 0.5-5.0 mA, no flux is admitted into the link system (perfect Meissner state). Above the critical current, flux is admitted in discrete quanta known as vortices(6). These vortices can move (flow) due to the Lorentz-type force generated by the bias current. In terms of active device performance, the key principle is the use of an external magnetic field (via the control line) to modulate the flux density in the link system (7),(8), the resulting flux motion and hence the terminal voltage.

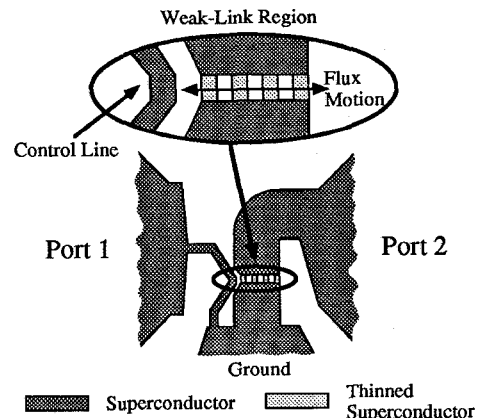
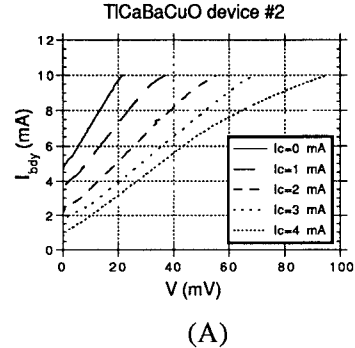


Figure 1. Layout of the Superconducting Flux Flow Transistor, Port 1 is the control line and port 2 is the device body. The connections shown taper into coplanar waveguides where contact is then made.

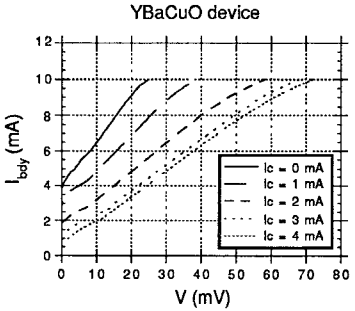
Devices have been made from films of TlCaBaCuO and YBaCuO on LaAlO₃ substrates. The TlCaBaCuO films were made by sequential e-beam evaporation followed by sintering in air under a partial pressure of Tl-O and annealing in oxygen. The process is described in detail elsewhere (9). The Tl samples used in these experiments had T_c's of about 103K and critical current densities at 77K (0 field) of about 350 kA/cm². In making the YBaCuO films, Y and Cu metals are evaporated from separate electron gun sources and BaF₂ is resistively evaporated (10). The films are annealed ex-situ in a carefully optimized multi-stage process (11). The YBCO films used in these experiments had T_c's of about 90K and critical current densities at 77K (0 field) of about 1 MA/cm².

I-V curves for two of the devices (one made of TlCaBaCuO and one of YBaCuO) tested are shown in Fig. 2. The current through the link system (or body) is denoted by I_{bdy} while the control current is labeled I_c. The two most important circuit parameters to be drawn from these curves are the transresistance ($r_m = \Delta V / \Delta I_c$) and output resistance ($r_o = \Delta V / \Delta I_{bdy}$). For the microwave measurements, the devices will be biased I_{bdy}=8 mA and I_c=0.2 mA where typical values are $r_m \approx 17-19 \Omega$ and $r_o \approx 3-4 \Omega$. An equivalent circuit based on device physics is shown in Fig. 3 (5). Since moving flux generates a voltage and the impetus is a control current, a transresistance is the active element for the equivalent circuit. The moving vortices have normal cores and hence represent an ohmic resistance (r_o). The input and output impedances are both inductive because of the geometry of the structures and, for the output inductance, because of the excess kinetic inductance of the thin superconducting film in the link region(12).

NN



(A)



(B)

Figure 2. IV curves of two SFFT's (a) a TlCaBaCuO device, (b) a YBaCuO device. I_{bdy} is the current through the device body (link region) and I_c is the control current. The voltage V is measured across the link system.

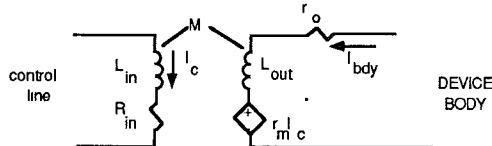
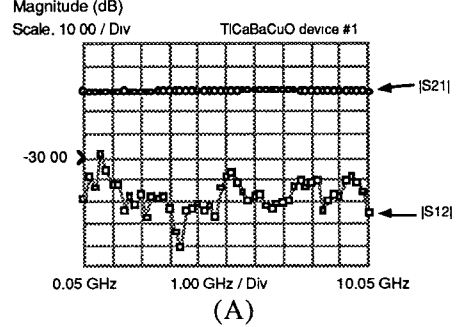


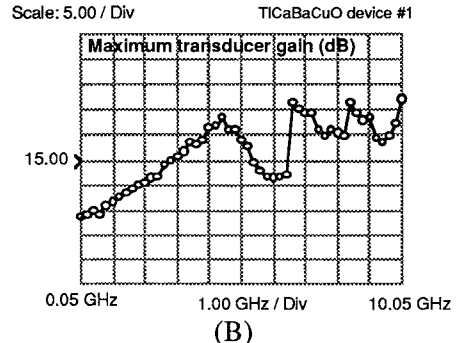
Figure 3. An equivalent circuit of the SFFT. Values of the components are discussed in the text. The transresistance component is the active element. Other interesting features include the non-linearity of the output inductor and the low amount of cross-talk (M is typically 10 pH).

S-PARAMETER MEASUREMENTS

The first measurements were made with Cascade signal-ground probes using SOTL (short, open, thru, load) calibration (13). This probing scheme presented problems because of planarity requirements and the irregularity of the LaAlO_3 substrates used. As a result, contacting was difficult. Data were obtained for one Tl device at 77K with some effort and these results are summarized in Fig. 4. The roughness of the maximum transducer gain (MTG) (14) is due largely to unstable contacts (particularly in the liquid nitrogen environment). There are, however, some interesting features of these data. S_{21} is reasonably large in magnitude and $|S_{21}| \gg |S_{12}|$ indicating active behavior. The measurement of these two parameters was relatively repeatable (to within ~ 1 dB) and at least semi-quantitatively correct since an unbiased device showed $|S_{12}| = |S_{21}| \sim -40$ dB across the band. The MTG, while having some uncertainty, does indicate the possibility of large gain with adequate matching.



(A)



(B)

Figure 4. Measured S-parameters (a) and computed Maximum transducer gain (b) for a Tl SFFT probed with Cascade signal-ground probes. Note the low cross-talk and large available gain. The roughness of MTG is due to contacting problems. For all MTG plots, maximum available gain is used when the device is stable and maximum stable gain is used otherwise.

Custom probes using Cascade mounts and spring-loaded pogo launchers in a ground-signal-ground configuration were designed to circumvent contacting problems. These probes, though still not perfected, did allow for highly repeatable measurements below 10 GHz. Dual-band TRL (thru, short, delay) calibration (13) at 77K was employed. The 77K S-parameters for the two devices (whose IV curves are in Fig. 2) are shown in Fig. 5. The bias point ($I_{bdy}=8$ mA, $I_c=0.2$ mA) was chosen because r_m was nearing its plateau value and r_o was still relatively small. S_{21} behaves as with the device of Fig. 4 but $|S_{12}|$ is larger. This is largely due to poor isolation with our present probe design. To verify the isolation problem, both probes were placed on a shorting block about the same distance apart from each other as during the transistor measurement and the S-parameters were measured. The measured $|S_{12}|$ and $|S_{21}|$ are shown in Fig. 6 and indicate the poor isolation which is undoubtedly masking the true transistor S_{12} . The actual device S_{12} is probably like that shown in Fig. 4. MTG calculations are shown in Fig. 7 (using the actual measured device data). Even with the S_{12} error, the MTG exceeds 14 dB. We expect 20-25 dB is closer to the actual MTG over this band.

Model parameters can be determined by fitting the equivalent circuit to the data of Fig. 5. After removing launch parasitics (obtained by looking at a device electrode configuration with no SFFT in place), the equivalent circuit of Fig. 3 was fit to the data for the YBCO device (Fig. 5b). The control line was found to be adequately modeled by a 0.3 nH input inductance and an input resistance of 0.2 Ω . The other model parameters include $r_m \approx 18.2 \Omega$, $r_o \approx 3.7 \Omega$, and $L_{out} \approx 0.17$ nH. This fitting process was repeated for the Tl device at different bias levels and the results are shown in Table 1. As is apparent, the output resistance, transresistance, and output

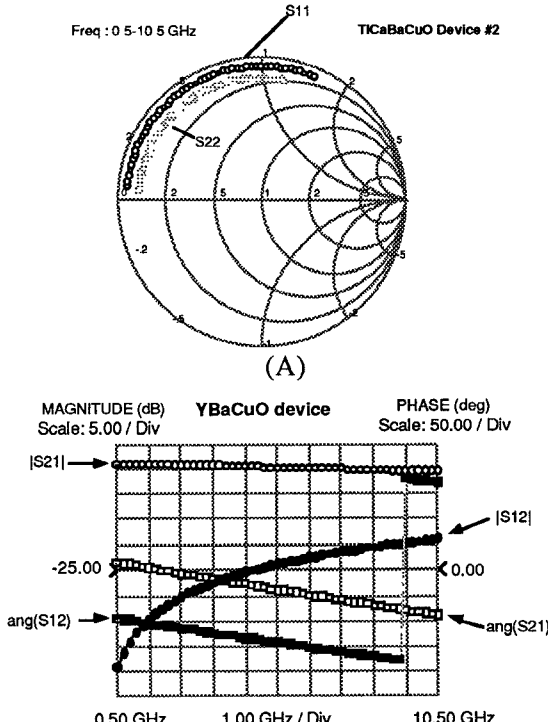
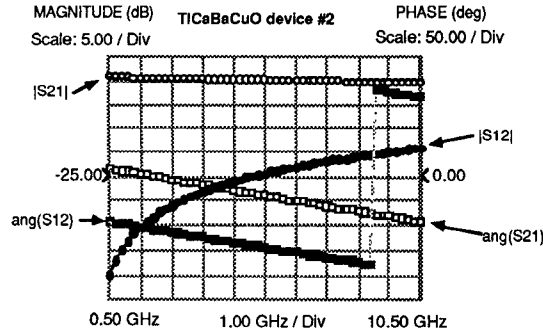


Figure 5. Measured S-parameters of a TiCaBaCuO device (a) and a YBaCuO device (b) probed using the spring-loaded structure described in the text. In both cases, the bias conditions were $I_{bdy}=8.0$ mA and $I_c=0.2$ mA. The data show inductive input and output impedances (low in magnitude) and a higher $|S_{21}|$ due largely to the probes.

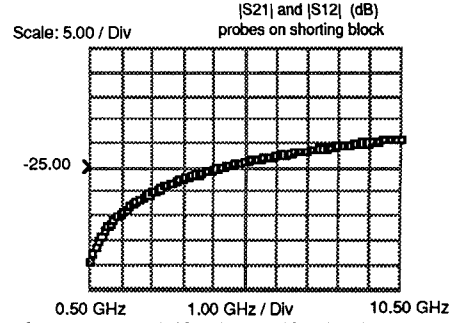


Figure 6. Measured $|S_{21}|$ and $|S_{12}|$ of the two probes (spring-loaded) placed on a shorting block separated by the spacing used in the Fig. 5 experiments. This shows that the true $|S_{12}|$ of the devices is probably no higher than that shown in Fig. 4.

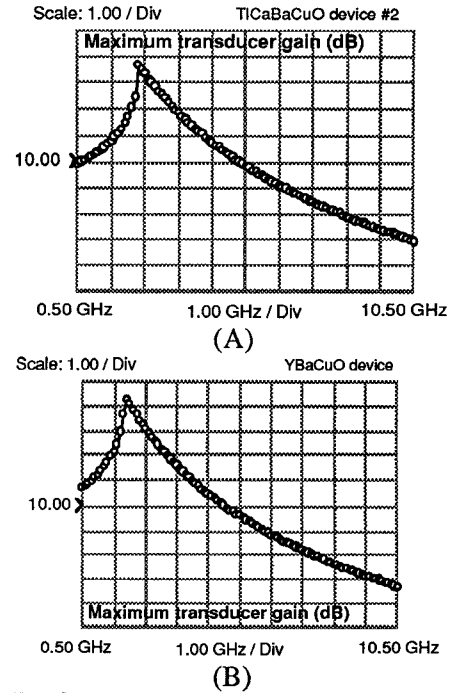


Figure 7. Computed Maximum Transducer Gain of the devices measured for Fig. 5. (a) TiCaBaCuO device and (b) YBaCuO device. Even with the error in S_{12} , the MAG exceeds 13 dB.

inductance are all reasonably strong functions of bias. The transresistance reaches a relatively broad plateau while the output resistance and inductance are somewhat more volatile. The dependence of the output inductance on control current is suitable for phase shifting. The effect of changing control current is qualitatively similar to that of changing the body current since in both cases local fields are being modified. The quantitative changes are different because of the control field anisotropy and screening currents generated.

I_{bdy} (mA)	I_c (mA)	r_m (Ω)	r_o (Ω)	L_{out} (nH)	L_{in} (nH)	R_{in} (Ω)
6.0	0.2	10.2	3.9	0.65	0.3	0.1
8.0	0.2	17.8	4.0	0.49	0.3	0.1
10.0	0.2	18.0	4.5	0.32	0.3	0.1
6.0	2.5	6.8	9.3	0.30	0.3	0.1
8.0	2.5	8.8	9.7	0.18	0.3	0.1
10.0	2.5	9.2	10.1	0.1	0.3	0.1

TABLE 1. Equivalent circuit parameter values for the device of Fig. 5a at various bias levels. Note the variability of the output inductance and resistance and the plateau that r_m quickly reaches.

AN APPLICATION

Because of the relatively large transresistance and low impedances, a matched amplifier could show very high gains(4). The most recent results are shown in Fig. 8 using the device of Fig. 5b. A maximum gain of about 13 dB was achieved with a return loss of 9 dB at midband. The matching attempt was not to achieve MTG but to get as much gain as possible with about 1 GHz of bandwidth and a center frequency of about 4 GHz. The matching in this case was done with normal transmission line sections for convenience but superconducting matching networks have been used previously (4) and have insertion loss advantages. Since the impedance mismatch is rather severe, relatively high currents will be flowing on the device side of the matching net and any normal conductor losses will become significant.

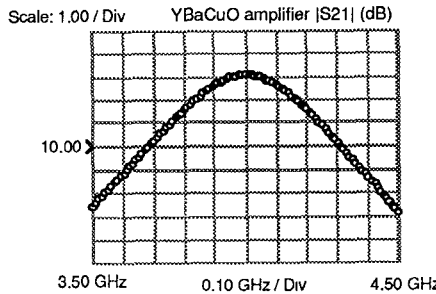


Figure 8. Performance of a matched amplifier constructed with the device of Fig. 5b. Maximum gain of 13 dB was achieved with a bandwidth of almost 1 GHz.

CONCLUSIONS

We have presented S-parameter measurements of a superconducting flux flow transistor. They indicate that are large amount of power gain is available but significant matching must be employed. An example was given showing an amplifier with over 13 dB gain a bandwidth of roughly 1 GHz at a center frequency of 4 GHz. Multistage and distributed structures are currently being investigated. Other applications including synthetic transmission line phase shifters (using the SFFT's variable output inductance), active impedance convertors (3) and mixers (5) have been successfully tried as well.

ACKNOWLEDGEMENTS

This work was supported by the U.S. Department of Energy through Sandia National Laboratories under contract No. DE-AC04-76P00789 and by DARPA, ONR and SDI under contract No. N0017390WR00172. The authors would like to thank Gert Hohenwarter of the University of Wisconsin-Madison and Parkview Works of Milton, WI for motivating some of the probing techniques and for useful discussions.

REFERENCES

- (1) G. K. G. Hohenwarter, J. S. Martens, D. P. McGinnis, J. B. Beyer, J. E. Nordman, and D. S. Ginley, "Single superconducting thin film devices for applications in high T_c materials circuits," IEEE Trans. on Mag., vol. MAG-25, pp. 954-956: Mar 1989.
- (2) J. S. Martens, G. K. G. Hohenwarter, J. B. Beyer, J. E. Nordman, and D. S. Ginley, "S parameter measurements on single superconducting thin-film three-terminal devices made of high- T_c and low T_c materials," J. Appl. Phys., vol. 65, pp. 4057-4060: May 1989.
- (3) J. S. Martens, J. B. Beyer, J. E. Nordman, G. K. G. Hohenwarter and D. S. Ginley, "A Josephson Junction to FET High Speed Line Driver made of Ti-Ca-Ba-Cu-O," to be published in IEEE Trans. on Mag., vol. MAG-27: Mar 1991.
- (4) G. K. G. Hohenwarter, J. S. Martens, J. B. Beyer and J. E. Nordman, "Resonant Impedance Matching of Abrikosov Vortex-Flow Transistors," to be published in IEEE Trans. on Mag., vol. MAG-27: Mar 1991.
- (5) J. S. Martens, "The Model and Applications of a High Frequency Three Terminal Device Made of High Temperature Superconductors," PhD Dissertation, University of Wisconsin-Madison: May 1990.
- (6) K. K. Likharev, "Vortex motion and the Josephson effect in superconducting thin bridges," Sov. Phys. - JETP, vol. 34, pp. 906-912: Apr 1972.
- (7) T. Van Duzer and C. W. Turner, Principles of Superconductive Devices and Circuits, New York: Elsevier, 1981, Chp. 8.
- (8) J. Pearl, "Current distribution in superconducting films carrying quantized fluxoids," Appl. Phys. Lett., vol. 5, pp. 65-66: Jul 1964.
- (9) D. S. Ginley, J. F. Kwak, E. L. Venturini, B. Morosin and R. J. Baughman, "Morphology control and high critical currents in superconducting thin films in the Ti-Ca-Ba-Cu-O system," Physica C, Vol. 160, pp. 42-48: Oct 1989.
- (10) M. P. Siegal, J. M. Phillips, Y. F. Hsieh and J. H. Marshall, "Growth of epitaxial $Ba_2YCu_3O_{7-x}$ films on $LaAlO_3$ (001)," Physica C, vol. 172, pp. 282-286: Dec 1990.
- (11) M. P. Siegal, J. M. Phillips, R. B. van Dover, T. H. Tiefel and J. H. Marshall, "Optimization of annealing parameters for the growth of epitaxial $Ba_2YCu_3O_{7-x}$ films on $LaAlO_3$ (001)," J. Appl. Phys., vol. 68, pp. 6353-6360: Dec 1990.
- (12) T. Van Duzer and C. W. Turner, Principles of Superconductive Devices and Circuits, New York: Elsevier, 1981, Chp. 3.
- (13) "On-wafer measurements using the HP 8510 network analyzer and Cascade Microtech wafer probes," Hewlett Packard, Product Note 8510-6, 1986.
- (14) G. Gonzalez, Microwave Transistor Amplifiers, Englewood Cliffs, NJ: Prentice-Hall, 1984, Chp. 3.